Journal of Physics G: Nuclear and Particle Physics



# DREENA-C framework: joint $R_{AA}$ and $v_2$ predictions and implications to QGP tomography

OPEN ACCESS
IOP Publishing
Journal of Physics G: Nuclear and Particle Physics
J. Phys. G: Nucl. Part. Phys. **46** (2019) 085101 (13pp)
https://doi.org/10.1088/1361-6471/ab2356

# DREENA-C framework: joint $R_{AA}$ and $v_2$ predictions and implications to QGP tomography

**Dusan Zigic[1], Igor Salom[1], Jussi Auvinen[1], Marko Djordjevic[2] and Magdalena Djordjevic[1,3]**

[1] Institute of Physics Belgrade, University of Belgrade, Belgrade, Serbia
[2] Faculty of Biology, University of Belgrade, Belgrade, Serbia

E-mail: magda@ipb.ac.rs

Received 26 November 2018, revised 7 May 2019
Accepted for publication 21 May 2019
Published 26 June 2019

**Abstract**

In this paper, we presented our recently developed Dynamical Radiative and Elastic ENergy loss Approach (DREENA-C) framework, which is a fully optimized computational suppression procedure based on our state-of-the-art dynamical energy loss formalism in constant temperature finite size QCD medium. With this framework, we have generated, for the first time, joint $R_{AA}$ and $v_2$ predictions within our dynamical energy loss formalism. The predictions are generated for both light and heavy flavor probes, and different centrality regions in Pb + Pb collisions at the LHC, and compared with the available experimental data. While $R_{AA}$ predictions agree with experimental data, $v_2$ predictions qualitatively agree with, but are quantitatively visibly above, the experimental data (in disagreement with other models, which underestimate $v_2$). Consistently with numerical predictions, through simple analytic analysis, we show that $R_{AA}$ is insensitive to medium evolution (though highly sensitive to energy loss mechanisms), while $v_2$ is highly sensitive to the evolution. As a major consequence for precision quark-gluon plasma (QGP) tomography, this then leaves a possibility to calibrate energy loss models on $R_{AA}$ data, while using $v_2$ to constrain QGP parameters that are in agreement with both high and low $p_\perp$ data.

[3] Author to whom correspondence should be addressed.

Keywords: quark-gluon plasma, parton energy loss, heavy quarks, perturbative QCD, QGP tomography, high pt suppression predictions

(Some figures may appear in colour only in the online journal)

## 1. Introduction

Quark-gluon plasma (QGP) is a new state of matter [1, 2] consisting of interacting quarks, antiquarks and gluons. Such a new state of matter is created in ultra-relativistic heavy ion collisions at Relativistic Heavy Ion Collider (RHIC) and Large Hadron Collider (LHC). Rare high momentum probes, which are created in such collisions and which transverse QGP, are excellent probes of this extreme form of matter [3–5]. Different observables (such as angular averaged nuclear modification factor $R_{AA}$ and angular anisotropy $v_2$), together with probes with different masses, probe this medium in a different manner. Therefore, comparing comprehensive set of joint predictions for different probes and observables, with available experimental data from different experiments, collision systems and collision energies, allows investigating properties of QCD medium created in these collisions [6–12].

However, to implement this idea, it is necessary to have a model that realistically describes high-$p_\perp$ parton interactions with the medium. With this goal in mind, we developed state-of-the-art dynamical energy loss formalism [13, 14], which includes different important effects (some of which are unique to this model). Namely, (i) the formalism takes into account finite size, finite temperature QCD medium consisting of dynamical (that is moving) partons, contrary to the widely used static scattering approximation and/or medium models with vacuum-like propagators. (ii) The calculations are based on the finite temperature field theory [15, 16], and generalized HTL approach, in which the infrared divergencies are naturally regulated, so the model does not have artificial cutoffs. (iii) Both radiative [13] and collisional [17] energy losses are calculated under the same theoretical framework, applicable to both light and heavy flavor. (iv) The formalism is generalized to the case of finite magnetic [18] mass and running coupling [19], and most recently, we also applied first steps towards removing widely used soft-gluon approximation from radiative energy loss calculations, enhancing the applicability region of this formalism [20]. This formalism was further integrated into numerical procedure [19], which includes initial $p_\perp$ distribution of leading partons [21, 22], energy loss with path-length [23, 24] and multi-gluon [25] fluctuations, and fragmentation functions [26–28], to generate the final medium modified distribution of high $p_\perp$ hadrons. While all the above effects have to be included based on theoretical grounds, it is plausible to ask whether all of these ingredients are necessary for accurately interpreting the experimental data, particularly since other available approaches [29–33] commonly neglect some—or many—of these effects. To address this important issue, in [34], we showed that, while abolishing widely used static approximation is the most important step for accurate suppression predictions, *including all other effects* is necessary for a fine agreement with high-$p_\perp$ $R_{AA}$ (and $v_2$, not published) data.

To be able to generate predictions that can reasonably explain the experimental data, all ingredients stated above have to be preserved (with no additional simplifications used in the numerical procedure), as all of these ingredients were shown to be important for reliable theoretical predictions of jet suppression [34]. From computational perspective, it is also necessary to develop a framework that can efficiently generate wide set of theoretical predictions, to be compared with a broad range of available (or upcoming) experimental data. We here present DREENA-C (Dynamical Radiative and Elastic ENergy loss Approach) framework, which is the first step towards this goal. Due to the complexity of the underlying parton-medium

interaction model, this first step takes into account the medium evolution in its simplest form, through mean (constant) medium temperature (thus 'C' in DREENA-C framework). In addition to presenting the necessary baseline to be compared with future redevelopments of the dynamical energy loss to more fully account for the medium evolution, DREENA-C is also an optimal numerical framework for studying the medium evolution effects on certain observables. That is, as this framework takes into account state-of-the-art parton-medium interaction model, but only rudimental medium evolution, comparison of its predictions with experimental data allows assessing sensitivity of certain variables to QGP evolution.

DREENA-C framework corresponds to, in its essence, the numerical procedure presented in [19], with a major new development that the code is now optimized to use minimal computer resources and produce predictions within more than two orders of magnitude shorter time compared to [19]. Such step is necessary, as all further improvements of the framework, necessarily need significantly more computer time and resources. So, without this development, further improvements, e.g. towards nontrivially evolving QGP medium, would not be realistically possible. That is, DREENA-C framework, addresses the goal of efficiently generating predictions for diverse observables.

Exploiting the ability to generate predictions for a wide range of observables, we will here use DREENA-C framework to, for the first time, present joint $R_{AA}$ and $v_2$ theoretical predictions within our dynamical energy loss formalism; these predictions will be generated for different experiments (ALICE, CMS and ATLAS), probes (light and heavy) and experimental conditions (wide range of collision centralities). Note that some of our results correspond to true predictions (some centrality intervals for B and D mesons), while for other cases, e.g. for charged hadrons, they correspond to postdictions, as the experimental data are already available. Motivation for generating these predictions is the following: (i) the theoretical models up to now were not able to jointly explain these data, which is known as $v_2$ puzzle [35, 36]. That is, the models lead to underprediction of $v_2$, unless new phenomena (e.g. magnetic monopoles) are introduced [37]. (ii) Having this puzzle in mind, and the fact that other available models employ the complementary approach, i.e. combine simplified energy loss models with more sophisticated medium evolutions, this work will enable assessing to what extent state-of-the-art energy loss model, but with simplest QGP evolution, is able to jointly explain $R_{AA}$ and $v_2$ data. To obtain additional understanding of this important issue, we will bellow complement DREENA-C predictions with analytical estimates. (iii) DREENA-C predictions will establish an important baseline for testing how future introduction of the medium evolution will improve the formalism. Moreover, such step-by-step introduction of different medium evolution effects in the model will also allow to investigate their importance in explaining the experimental data, which is highly relevant for QGP tomography.

## 2. Methods

The DREENA-C framework is a fully optimized numerical procedure, which contains all ingredients presented in detail in [19]. We below briefly outline the main steps in this procedure.

The quenched spectra of light and heavy flavor observables are calculated according to the generic pQCD convolution:

$$\frac{E_f \mathrm{d}^3\sigma}{\mathrm{d}p_f^3} = \frac{E_i \mathrm{d}^3\sigma(Q)}{\mathrm{d}p_i^3} \otimes P(E_i \to E_f) \otimes D(Q \to H_Q). \tag{1}$$

Subscripts $i$ and $f$ correspond, respectively, to 'initial' and 'final', and $Q$ denotes initial light or heavy flavor jet. $E_i \mathrm{d}^3\sigma(Q)/\mathrm{d}p_i^3$ denotes the initial momentum spectrum, which are computed

according to [21, 22], $P(E_i \rightarrow E_f)$ is the energy loss probability, computed within the dynamical energy loss formalism [13, 14], with multi-gluon [25], path-length fluctuations [24] and running coupling [19]. $D(Q \rightarrow H_Q)$ is the fragmentation function of light and heavy flavor parton $Q$ to hadron $H_Q$, where for light flavor, D and B mesons we use, DSS [26], BCFY [27] and KLP [28] fragmentation functions, respectively.

Regarding the numerical procedure, a major new development is that the code is now optimized, so that it is two orders of magnitude faster compared to the brute-force approach applied in [19]. Technically, the main optimization method we used was a combination of tabulation and interpolation of values of intermediary functions that appear at various steps of the energy loss calculation. This approach significantly reduces the number of necessary integrations. However, it must be preceded by careful analysis of the behavior of interpolated functions and the function sampling must be tailored to this behavior, so that effectively no loss of precision is introduced. Furthermore, in comparison to the computation of [19], different and better suited methods of numerical integration were used (mostly quasi Monte Carlo integration), producing a large speedup, higher integration precision and stability of the underlying results. Finally, the code was parallelized to take advantage of contemporary multi-core workstations. Furthermore, the optimization also allowed for further improvements of the physical model: (i) due to numerical constraints, in the previous multi-gluon fluctuation procedure, the number of radiated gluons was limited to 3. The procedure is now redeveloped to include the arbitrary number of radiated gluons; the detailed numerical analysis (both from the point of numerical precision and time efficiency) showed that the optimal limit of gluons to be included in the procedure is 4–5. (ii) Both radiative and collisional energy losses are now combined gradually along the traversed path of the parton, unlike in [19], where radiative and collisional losses were accounted separately.

As noted above, we model the medium by assuming a constant average temperature of QGP. We concentrate on the central rapidity region in 5.02 TeV Pb + Pb collisions at the LHC, though we note that these predictions will be applicable for 2.76 TeV Pb + Pb collisions as well, since the predictions for these two collision energies almost overlap [38]. To determine the temperature for each centrality region in 5.02 TeV Pb + Pb collisions, we use [39, 40] $T^3 \sim \frac{\frac{dN_g}{dy}}{A_\perp \overline{L}} \rightarrow T = c\left(\frac{\frac{dN_{ch}}{dy}}{A_\perp \overline{L}}\right)^{1/3}$, where $\frac{dN_g}{dy}$ is gluon rapidity density, $A_\perp$ is the overlap area and $\overline{L}$ is the average size of the medium for each centrality region. At mid rapidity, $\frac{dN_g}{dy}$ is directly proportional to experimentally measured charged particle multiplicity $\frac{dN_{ch}}{d\eta}$, which is measured for 5.02 TeV Pb + Pb collisions at the LHC across different centralities [41]. Furthermore, $c$ is a constant, which can be fixed through ALICE measurement of effective temperature for 0%–20% centrality at 2.76 TeV Pb + Pb collisions LHC [42]. For each centrality region, path-length distributions (as well as overlap area $A_\perp$ and average size of the medium $\overline{L}$) are calculated following the procedure described in [23], with an additional hard sphere restriction $r < R_A$ in the Woods–Saxon nuclear density distribution to regulate the path lengths in the peripheral collisions.

In numerical calculations, we use no fitting parameters in generating predictions for comparison with the data, i.e. all the parameters correspond to standard literature values. We consider a QGP with $\Lambda_{\rm QCD} = 0.2$ GeV and $n_f = 3$. The temperature dependent Debye mass $\mu_E$ $(T)$ is obtained from [43], while for the light quarks, we assume that their mass is dominated by the thermal mass $M \approx \mu_E/\sqrt{6}$, and the gluon mass is $m_g \approx \mu_E/\sqrt{2}$ [44]. The charm (bottom) mass is $M = 1.2$ GeV ($M = 4.75$ GeV). Finite magnetic mass effect is also included in our framework [18], as various non-perturbative calculations [45, 46] have shown that magnetic mass $\mu_M$ is different from zero in QCD matter created at the LHC and RHIC.

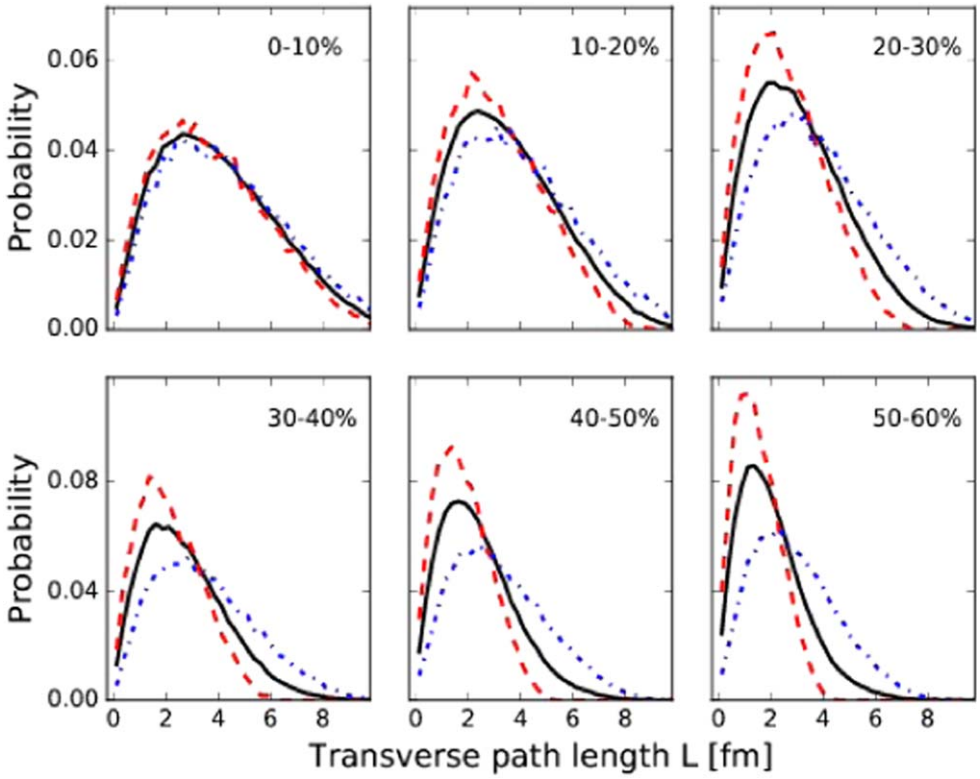


**Figure 1.** Path-length distributions. Probability distributions for hard parton path lengths in Pb + Pb collisions at $\sqrt{s_{NN}} = 5.02$ TeV for (0–10)%–(50–60)% centrality classes. Solid black curves: the total distributions with all hard partons included are represented; Dashed red curves: the distributions include only in-plane particles ($|\phi| < 15^\circ$ or $||\phi| - 180^\circ| < 15^\circ$); dashed–dotted blue curves: the distributions include only out-of-plane partons ($||\phi| - 90^\circ| < 15^\circ$).

Magnetic to electric mass ratio is extracted from these calculations to be $0.4 < \mu_M/\mu_E < 0.6$, so presented uncertainty in the predictions comes from this range of screening masses ratio. Note that other uncertainties (e.g. in quark masses or effective temperature), are not included in this study. However, we have checked that uncertainties in the quark masses lead to small (up to 4% for $p_\perp > 8$ GeV, and decreasing with increasing $p_\perp$) difference in the resulting predictions. Regarding effective temperature, as this temperature comes with large error bars, in [47] we presented a detailed study of how this uncertainty affects the $R_{AA}$ calculations. We found that $R_{AA}$ dependence on $T$ is almost linear (and the same for all parton energies and all types of flavor) and does not significantly affect the suppression, concluding that uncertainty in the effective temperature would basically lead to a systematic (constant value) shift in the predictions, i.e. the results presented in this paper would not be affected by this uncertainty.

## 3. Results and discussion

In this section, we will present joint $R_{AA}$ and $v_2$ predictions for high $p_\perp$ charged hadrons, D and B mesons in Pb + Pb collisions at the LHC. In figure 1 we first show probability

distributions for hard parton path lengths in Pb + Pb collisions for different centralities, obtained by the procedure specified in the previous section. For most central collisions, we observe that in-plane and out-of-plane distributions almost overlap with the total (average) path-length distributions, as expected. As the centrality increases, in-plane and out-of-plane distributions start to significantly separate (in different directions) from average path-length distributions. Having in mind that [48]

$$v_2 \approx \frac{1}{2}\frac{R_{AA}^{\text{in}} - R_{AA}^{\text{out}}}{R_{AA}^{\text{in}} + R_{AA}^{\text{out}}}, \tag{2}$$

this leads to the expectation of $v_2$ being small in most central collisions and increasing with increasing centrality. Regarding the equation (2) above, note that this estimate presents a conventional way [48–51] to calculate high $p_\perp$ $v_2$, and it leads to exact result if the higher harmonics $v_4$, $v_6$, etc. are zero at high $p_\perp$, and the opening angle (where $R_{AA}^{\text{in}}$ and $R_{AA}^{\text{out}}$ are evaluated) goes to zero.

Based on path-length distributions from figure 1, we can now calculate average $R_{AA}$, as well as in-plane and out-of-plane $R_{AA}$s ($R_{AA}^{\text{in}}$ and $R_{AA}^{\text{out}}$), and consequently $v_2$ for both light and heavy flavor probes and different centralities. We start by generating predictions for charged hadrons, where data for both $R_{AA}$ and $v_2$ are available. Comparison of our joint predictions with experimental data is shown in figure 2, where left and right panels correspond, respectively, to $R_{AA}$ and $v_2$. We see good agreement with $R_{AA}$ data, which is also robust, i.e. achieved across wide range of centralities and experiments. Regarding $v_2$, we surprisingly see that our $v_2$ predictions are visibly above the data. This is in contrast with other energy loss models which consistently lead to underprediction of $v_2$, where to resolve this, new phenomena (e.g. magnetic monopoles) were introduced [37]. Despite this quantitative disagreement, we see a reasonable qualitative agreement between the model and the data, i.e. the predictions are just shifted above the data; this will be further discussed below.

In figure 3, we provide predictions for D meson average $R_{AA}$ (left panel) and $v_2$ (right panel) data, for four different centrality regions. The predictions are compared with the available 5.02 TeV Pb + Pb experimental data. For average $R_{AA}$, we observe good agreement with the data. Regarding $v_2$, we observe similar behavior as for charged hadron: i.e. while we obtain a reasonable qualitative agreement with the measurements, quantitatively there is again an unexpected (having in mind predictions of other models) overestimation of the data. Figure 4 shows equivalent predictions as figure 3, only for B mesons. For $R_{AA}$, we compare our predictions with the available $B^{\pm}$ [58], $B_s^0$ [59], non-prompt $J/\Psi$ [60, 61] and non-prompt $D_0$ [62] data. Note that we can compare B meson predictions with these indirect b quark suppression data, as due to interplay of collisional and radiative energy loss, B meson suppression is almost independent on $p_\perp$ for $p_\perp > 10\,\text{GeV}$ [47], so the fragmentation/decay functions will not play a large role for different types of b quark observables. Also, note that our predictions are provided for mid-rapidity region; for non-prompt $D_0$ (which are given for $|y < 1|$), we see good agreement between our predictions and the data. For $B^{\pm}$ and non-prompt $J/\Psi$, our predictions show qualitatively good agreement, but overprediction of $R_{AA}$ data. This is expected, having in mind that those data are given for $|y \lesssim 2|$, where both experiments show 30%–50% increase in $R_{AA}$ with decreasing rapidity. Our predictions do not agree with $B_s^0$, but these data come with very large error bars. For $v_2$, we predict values significantly different from zero for all centrality regions, and see that our predictions agree with the available non-prompt $J/\Psi$ data [61, 63], though we note that these predictions are given with very large error bars. This does not necessarily mean that heavy B meson flows, as flow is inherently connected with *low* $p_\perp$ $v_2$, and here we show predictions for high $p_\perp$. On

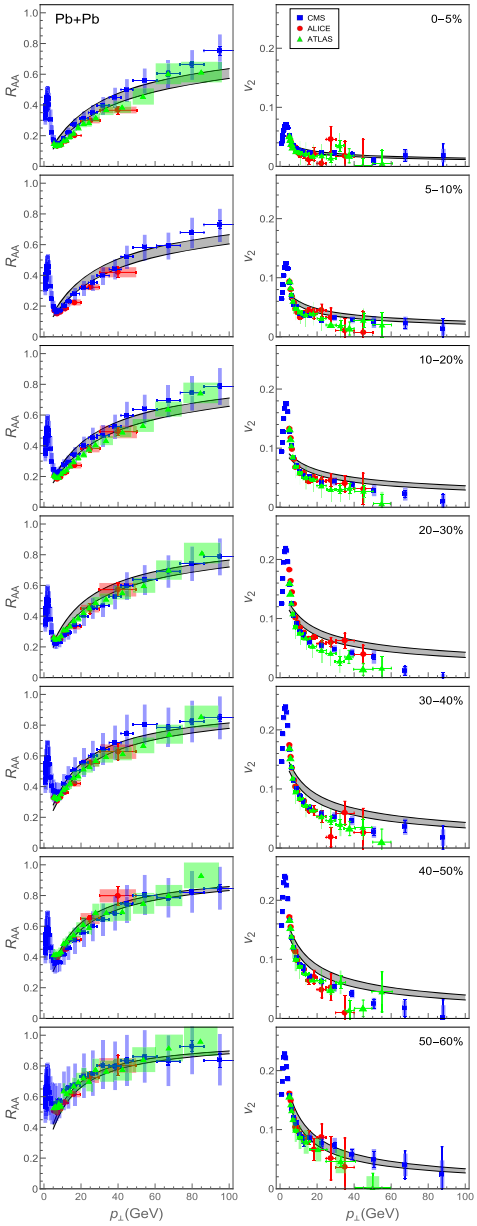


**Figure 2.** Joint $R_{AA}$ and $v_2$ predictions for charged hadrons. *Left panels:* theoretical predictions for $R_{AA}$ *versus* $p_\perp$ are compared with ALICE [52] (red circles), CMS [53] (blue squares) and ATLAS [54] (green triangles) charged hadron experimental data for 5.02 TeV Pb + Pb collisions at the LHC. *Right panels:* theoretical predictions for $v_2$ *versus* $p_\perp$ are compared with ALICE [55] (red circles), CMS [56] (blue squares) and ATLAS [57] (green triangles) charged hadron experimental data for 5.02 TeV Pb + Pb collisions at the LHC. The gray band boundaries correspond to $\mu_M/\mu_E = 0.4$ and $\mu_M/\mu_E = 0.6$. Rows 1–7 correspond to, respectively, 0%–5%, 5%–10%, 10%–20%,…, 50%–60% centrality regions.

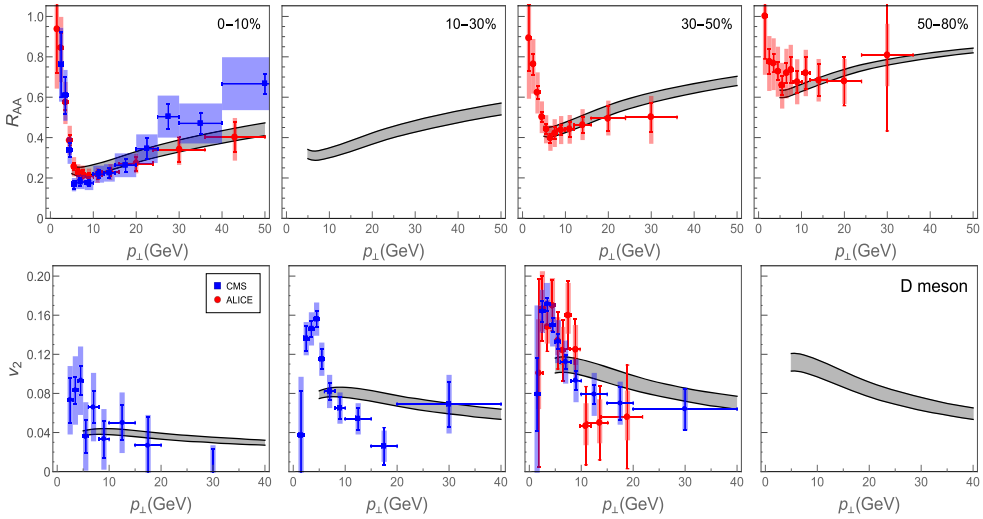


**Figure 3.** Joint $R_{AA}$ and $v_2$ predictions for D mesons. *Upper panels:* theoretical predictions for $R_{AA}$ *versus* $p_\perp$ are compared with ALICE [64] (red circles) and CMS [65] (blue squares) D meson experimental data for 5.02 TeV Pb + Pb collisions at the LHC. *Lower panels:* theoretical predictions for $v_2$ *versus* $p_\perp$ are compared with ALICE [51] (red circles) and CMS [66] (blue squares) D meson experimental data for 5.02TeV Pb + Pb collisions at the LHC. The gray band boundaries correspond to $\mu_M/\mu_E = 0.4$ and $\mu_M/\mu_E = 0.6$. First to fourth column correspond to, respectively, 0%–10%, 10%–30%, 30%–50% and 50%–80% centrality regions.

the other hand, high $p_\perp$ $v_2$ is connected with the difference in the energy loss (i.e. suppression) for particles going in different (e.g. in-plane and out-of-plane) directions; this difference then leads to our predictions of non-zero $v_2$ for *high* $p_\perp$ B mesons.

Overall, we see that our predicted $R_{AA}$s agree well with all measured (light and heavy flavor) data, while our $v_2$ predictions are consistently above the experimental data. Since our model has sophisticated description of parton-medium interactions, but highly simplified medium evolution model (through average medium temperature), these robust numerical results imply the following: (i) $R_{AA}$ is largely insensitive to the medium evolution, in contrast to its (previously shown [34]) large sensitivity to parton-medium interactions. (ii) $v_2$ is sensitive to the details of medium evolution. These two conclusions have important implications for QGP tomography, in particular (i) $R_{AA}$ can be used to calibrate parton-medium interaction models, while (ii) $v_2$ can be used to constrain QGP medium evolution parameters also from the point of high $p_\perp$ data (in addition to constraining them from low $p_\perp$ predictions/measurements). One should note that insensitivity of $R_{AA}$ and sensitivity of $v_2$ predictions to QGP evolution were also observed by using very different models and numerical frameworks [67, 68]. This then clearly suggests that such (in)sensitivity may be a general phenomenon, but to claim this, one should also gain an analytical understanding, which we provide below. Furthermore, the numerical results presented above also lead to the following questions, which are important from the point of future precision QGP tomography: (i) what is the reason behind the observed overestimation of $v_2$ within DREENA-C framework, and can expanding medium lead to a better agreement with the experimental data? (ii) Do we expect that B meson $v_2$ predictions will still be non-zero, once the expanding medium is introduced?

To intuitively approach the issues raised above, we start by noting that, within our dynamical energy loss formalism, $\Delta E/E \sim T^a$ and $\Delta E/E \sim L^b$, where $a, b \to 1$ ($\Delta E/E$ is

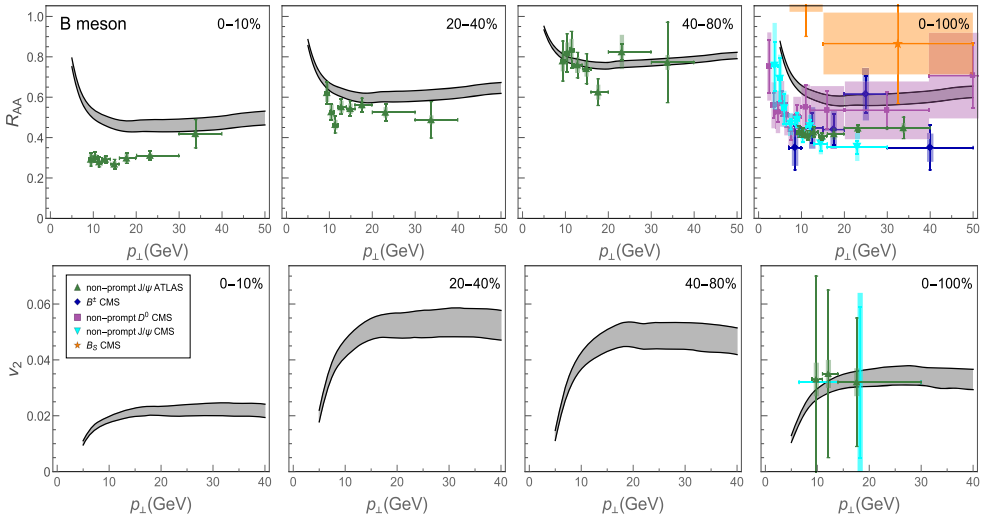


**Figure 4.** Joint $R_{AA}$ and $v_2$ predictions for B mesons. *Upper panels*: theoretical predictions for B meson $R_{AA}$ *versus* $p_\perp$ are compared with ATLAS [60] (green triangles), CMS [61] (cyan triangles) non-prompt $J/\Psi$, and CMS non-prompt $D^0$ [62] (purple squares), $B^\pm$ [58] (blue diamonds) and $B_s^0$ [59] (orange stars) experimental data for 5.02 TeV Pb + Pb collisions at the LHC. *Lower panels:* theoretical predictions for B meson $v_2$ *versus* $p_\perp$ are compared with ATLAS [63] (green triangles) and CMS [61] (cyan triangles) non-prompt $J/\Psi$ for 5.02TeV Pb + Pb collisions at the LHC. The gray band boundaries correspond to $\mu_M/\mu_E = 0.4$ and $\mu_M/\mu_E = 0.6$. First to fourth column correspond to, respectively, 0%–10%, 20%–40%, 40%–80% and 0%–100% centrality regions.

fractional energy loss, $T$ is the average temperature of the medium, while $L$ is the average path-length traversed by the jet). To be more precise, note that both dependencies are close to linear, though $a$ and $b$ are still significantly different from 1 [38]. However, for the purpose of this estimate, let us assume that $a = b = 1$, leading to

$$\Delta E/E \approx \chi TL, \tag{3}$$

where $\chi$ is a proportionality factor.

Another commonly used estimate [25] is that

$$R_{AA} \approx \left(1 - \frac{1}{2}\frac{\Delta E}{E}\right)^{n-2}, \tag{4}$$

where $n$ is the steepness of the initial momentum distribution function (i.e. approximate exponent of a power-law of initial momentum distribution $p_\perp^{-n}$), and $\Delta E/E$ is notably smaller than 1.

In the case when fractional energy loss $\Delta E/E \ll 1$, equation (4) becomes

$$R_{AA} \approx \left(1 - \frac{n-2}{2}\frac{\Delta E}{E}\right) \approx (1 - \xi TL), \tag{5}$$

where $\xi = (n-2)\,\chi/2$.

In the DREENA-C approach, $T$ is constant, and the same in in-plane and out-of-plane directions, while $L_{\text{in}} = L - \Delta L$ and $L_{\text{out}} = L + \Delta L$, leading to

$$R_{AA} \approx \frac{1}{2}(R_{AA}^{\text{in}} + R_{AA}^{\text{out}}) \approx \frac{1}{2}(1 - \xi TL_{\text{in}} + 1 - \xi TL_{\text{out}}) = 1 - \xi T\frac{L_{\text{in}} + L_{\text{out}}}{2} = 1 - \xi TL, \tag{6}$$

and

$$v_2 \approx \frac{1}{2}\frac{R_{AA}^{\text{in}} - R_{AA}^{\text{out}}}{R_{AA}^{\text{in}} + R_{AA}^{\text{out}}} \approx \frac{1}{2}\frac{(1 - \xi TL_{\text{in}}) - (1 - \xi TL_{\text{out}})}{2(1 - \xi TL)} = \frac{1}{2}\frac{\xi T\Delta L}{1 - \xi TL} \approx \frac{\xi T\Delta L}{2}. \tag{7}$$

If the medium evolves, and by assuming 1 + 1D Bjorken time evolution [69] (as qualitatively sufficient for the early time dynamics [70]), the average temperature along in-plane will be larger than along out-of-plane direction [71], leading to $T_{\text{in}} = T + \Delta T$ and $T_{\text{out}} = T - \Delta T$ (where $\Delta L/L \cdot \Delta T/T \ll 1$). By repeating the above procedure in this case, it is straightforward to obtain

$$R_{AA} \approx 1 - \xi TL \tag{8}$$

and

$$v_2 \approx \frac{1}{2}\frac{(1 - \xi T_{\text{in}}L_{\text{in}}) - (1 - \xi T_{\text{out}}L_{\text{out}})}{2(1 - \xi TL)} = \frac{1}{2}\frac{\xi T\Delta L - \xi\Delta TL}{1 - \xi TL} \approx \frac{\xi T\Delta L - \xi\Delta TL}{2}. \tag{9}$$

We see that, while $v_2$ explicitly depends on $\Delta T$ and $\Delta L$, $R_{AA}$ does not. Therefore, it follows that, consistently with previous numerical results, $R_{AA}$ can be only weakly sensitive to QGP evolution, while $v_2$ is quite sensitive to this evolution; note that this is to our knowledge, the first time that analytical argument to sensitivity of $R_{AA}$ and $v_2$ to medium evolution is provided. Moreover, from equations (7) and (9), we see that introduction of temperature evolution is expected to lower $v_2$ compared to constant $T$ case. Consequently, an accurate/complete energy loss models, when applied in the context of constant temperature medium should lead to higher $v_2$ than expected, while introduction of $T$ evolution in such models would lower the $v_2$ compared to non-evolving case. Based on this, and the fact that previous theoretical approaches were not able to reach high enough $v_2$ without introducing new phenomena [37], we argue that accurate description of high-$p_\perp$ parton-medium interactions is crucial for accurate description of high-$p_\perp$ experimental data. With regards to this, the above results strongly suggest that the dynamical energy loss formalism has the right features needed to accurately describe jet-medium interactions in QGP, which is crucial for high precision QGP tomography.

Regarding the second question mentioned above, for B meson to have $v_2 \approx 0$, it is straightforward to see that one needs $\Delta T/T \approx \Delta L/L$. Having in mind that $\Delta L/L$ is quite large for larger centralities (see figure 1), $\Delta T/T$ would also have to be about the same magnitude. We do not expect this to happen, based on our preliminary estimates of the temperature changes in in-plane and out-of-plane in 1 + 1D Bjorken expansion scheme [69]. That is, our expectations is that B meson $v_2$ will be smaller than presented here, but still

significantly larger than zero, at least for large centrality regions. However, this still remains to be tested in the future with the introduction of full evolution model within our framework.

## 4. Conclusion

In this paper, we introduced the DREENA-C framework, which is a computational suppression procedure based on our dynamical energy loss formalism in finite size QCD medium with constant (mean) medium temperature. This approach, which combines a state-of-the-art energy loss model, but with including QGP evolution in its simplest form, is complementary to other available models that combine simplified energy loss models with more sophisticated medium evolutions. As such, DREENA-C can provide an important insight to what extent the accurate description of high-$p_\perp$ parton-medium interactions *versus* accurate description of medium evolution is necessary for accurately explaining high $p_\perp$ $R_{AA}$ and $v_2$ measurements.

We here used the DREENA-C framework to, for the first time, generate joint $R_{AA}$ and $v_2$ predictions for both light and heavy flavor probes and different centrality regions in Pb + Pb collisions at the LHC, and compare them with the available experimental data. We consistently, through both numerical and analytical calculations, obtained that $R_{AA}$ is sensitive to the average properties of the medium, while $v_2$ is highly sensitive to the details of the medium evolution. Analytical calculations brought another advantage of DREENA-C, as they would likely not be possible in frameworks with more complex medium evolution models, but bring simple and intuitive predictions/explanations for our results, which is necessary for better qualitative and quantitative understanding of the obtained results.

Since different medium evolution profiles have both different average properties and different details of the evolution, in precision QGP tomography, both $R_{AA}$ and $v_2$ have to be jointly used to extract the QGP properties. The DREENA-C framework presents an optimal starting point for QGP tomography, as $R_{AA}$ predictions (obtained through DREENA-C) can be first used to calibrate the energy loss model itself; that is, DREENA-C is fast (which is important for efficient energy loss calibration), and it does not contain the details of the medium evolution, which could provide an unwanted background for such a purpose. Once this crucial step of accurate description and calibration of parton-medium interactions is achieved, different more-detailed profiles of medium evolution (generated through different bulk medium models and parameters, with and without event by event fluctuations) can be tested (through our future advancement of DREENA framework) to assess which of these profiles provide a simultaneous agreement with both high $p_\perp$ $R_{AA}$ and $v_2$ data, across wide range of diverse experimental data and without further adjustment of energy loss models. In this way, QGP parameters can be constrained from both low and high $p_\perp$ measurements.

Furthermore, other approaches face difficulties in jointly explaining $R_{AA}$ and $v_2$ data, where smaller $v_2$, than experimentally observed, is obtained. In distinction to other approaches, we here obtained an overprediction of $v_2$, where the analytical estimates moreover show that inclusion of more realistic medium evolution models would lead to better agreement with the data. This, together with the fact that $v_2$ prediction provided here already qualitatively (though not quantitatively) agree with the data, indicate an important (and highly non-trivial) conclusion that accurate description of high-$p_\perp$ parton interactions with QGP is likely the most important ingredient for generating high-$p_\perp$ predictions. These results therefore strongly suggest that our dynamical energy loss formalism provides a suitable basis for the QGP tomography (outlined above), which is our main future goal.

## Acknowledgments

This work is supported by the European Research Council, grant ERC-2016-COG: 725741, and by the Ministry of Science and Technological Development of the Republic of Serbia, under project numbers ON171004, ON173052 and ON171031.

## ORCID iDs

Magdalena Djordjevic https://orcid.org/0000-0001-9229-4648

## References

[1] Collins J C and Perry M J 1975 *Phys. Rev. Lett.* **34** 1353
[2] Baym G and Chin S A 1976 *Phys. Lett.* B **62** 241
[3] Gyulassy M and McLerran L 2005 *Nucl. Phys.* A **750** 30
[4] Shuryak E V 2005 *Nucl. Phys.* A **750** 64
[5] Jacak B and Steinberg P 2010 *Phys. Today* **63** 39
[6] Bjorken J D 1982 FERMILAB-PUB-82-059-THY 287 292
[7] Djordjevic M, Gyulassy M and Wicks S 2005 *Phys. Rev. Lett.* **94** 112301
[8] Dokshitzer Yu L and Kharzeev D 2001 *Phys. Lett.* B **519** 199
[9] Burke K M *et al* (JET Collaboration) 2014 *Phys. Rev.* C **90** 014909
[10] Aarts G *et al* 2017 *Eur. Phys. J.* A **53** 93
[11] Akiba Y *et al* arXiv:1502.02730 [nucl-ex]
[12] Brambilla N *et al* 2014 *Eur. Phys. J.* C **74** 2981
[13] Djordjevic M 2009 *Phys. Rev.* C **80** 064909
[14] Djordjevic M and Heinz U 2008 *Phys. Rev. Lett.* **101** 022302
[15] Kapusta J I 1989 *Finite-Temperature Field Theory* (Cambridge: Cambridge University Press)
[16] Bellac M Le 1996 *Thermal Field Theory* (Cambridge: Cambridge University Press)
[17] Djordjevic M 2006 *Phys. Rev.* C **74** 064907
[18] Djordjevic M and Djordjevic M 2012 *Phys. Lett.* B **709** 229
[19] Djordjevic M and Djordjevic M 2014 *Phys. Lett.* B **734** 286
[20] Blagojevic B, Djordjevic M and Djordjevic M 2019 *Phys. Rev.* C **99** 024901
[21] Kang Z B, Vitev I and Xing H 2012 *Phys. Lett.* B **718** 482
[22] Sharma R, Vitev I and Zhang B W 2009 *Phys. Rev.* C **80** 054902
[23] Dainese A 2004 *Eur. Phys. J.* C **33** 495
[24] Wicks S, Horowitz W, Djordjevic M and Gyulassy M 2007 *Nucl. Phys.* A **784** 426
[25] Gyulassy M, Levai P and Vitev I 2002 *Phys. Lett.* B **538** 282
[26] de Florian D, Sassot R and Stratmann M 2007 *Phys. Rev.* D **75** 114010
[27] Cacciari M and Nason P 2003 *J. High Energy Phys.* JHEP09(2003)006
Braaten E, Cheung K-M, Fleming S and Yuan T C 1995 *Phys. Rev.* D **51** 4819
[28] Kartvelishvili V G, Likhoded A K and Petrov V A 1978 *Phys. Lett.* B **78** 615
[29] Baier R, Dokshitzer Yu L, Mueller A H, Peigne S and Schiff D 1997 *Nucl. Phys.* B **483** 291
Baier R, Dokshitzer Yu L, Mueller A H, Peigne S and Schiff D 1997 *Nucl. Phys.* B **484** 265
Zakharov B G 1996 *JETP Lett.* **63** 952
Zakharov B G 1997 *JETP Lett.* **65** 615
[30] Armesto N, Salgado C A and Wiedemann U A 2004 *Phys. Rev.* D **69** 114003
[31] Arnold P B, Moore G D and Yaffe L G 2001 *J. High Energy Phys.* JHEP11(2001)057
Arnold P B, Moore G D and Yaffe L G 2002 *J. High Energy Phys.* JHEP06(2002)030
Arnold P B, Moore G D and Yaffe L G 2003 *J. High Energy Phys.* JHEP01(2003)030
[32] Gyulassy M, Levai P and Vitev I 2001 *Nucl. Phys.* B **594** 371
Djordjevic M and Gyulassy M 2004 *Nucl. Phys.* A **733** 265–98
[33] Wang X N and Guo X F 2001 *Nucl. Phys.* A **696** 788
Majumder A and Leeuwen M Van 2011 *Prog. Part. Nucl. Phys.* A **66** 41
[34] Blagojevic B and Djordjevic M 2015 *J. Phys. G: Nucl. Part. Phys.* **42** 075105
[35] Noronha-Hostler J, Betz B, Noronha J and Gyulassy M 2016 *Phys. Rev. Lett.* **116** 252301

[36] Das S K, Scardina F, Plumari S and Greco V 2015 *Phys. Lett.* B **747** 260
[37] Xu J, Liao J and Gyulassy M 2015 *Chin. Phys. Lett.* **32** 092501
Shi S, Liao J and Gyulassy M 2018 *Chin. Phys.* C **42** 104104
[38] Djordjevic M and Djordjevic M 2015 *Phys. Rev.* C **92** 024918
[39] Gyulassy M, Levai P and Vitev I 2001 *Nucl.Phys.* B **594** 371
[40] Xu J, Buzzatti A and Gyulassy M 2014 *J. High Energy Phys.* JHEP08(2014)063
[41] Adam J *et al* (ALICE Collaboration) 2016 *Phys. Rev. Lett.* **116** 222302
[42] Adam J *et al* (ALICE Collaboration) 2016 *Phys. Lett.* B **754** 235
Wilde M and (for the ALICE Collaboration) 2013 *Nucl. Phys.* A **904-905** 573c
[43] Peshier A 2006 arxiv:hep-ph/0601119
[44] Djordjevic M and Gyulassy M 2003 *Phys. Rev.* C **68** 034914
[45] Yu Maezawa *et al* (WHOT-QCD Collaboration) 2010 *Phys. Rev.* D **81** 091501
[46] Nakamura A, Saito T and Sakai S 2004 *Phys. Rev.* D **69** 014506
[47] Djordjevic M 2016 *Phys. Lett.* B **763** 439
[48] Christiansen P, Tywoniuk K and Vislavicius V 2014 *Phys. Rev.* C **89** 034912
[49] Xu J, Buzzatti A and Gyulassy M 2014 *J. High Energy Phys.* JHEP08(2014)063
[50] Abelev B B *et al* (ALICE Collaboration) 2014 *Phys. Rev.* C **90** 034904
[51] Acharya S *et al* (ALICE Collaboration) 2018 *Phys. Rev. Lett.* **120** 102301
[52] Acharya S *et al* (ALICE Collaboration) 2018 *J. High Energy Phys.* JHEP11(2018)013
[53] Khachatryan V *et al* (CMS Collaboration) 2017 *J. High Energy Phys.* JHEP04(2017)039
[54] Aaboud M *et al* [ATLAS Collaboration] 2019 *Phys. Lett.* B **790** 108–28
[55] Acharya S *et al* (ALICE Collaboration) 2018 *J. High Energy Phys.* JHEP07(2018)103
[56] Sirunyan A M *et al* (CMS Collaboration) 2018 *Phys. Lett.* B **776** 195
[57] Aaboud M *et al* (ATLAS Collaboration) 2018 *Eur. Phys. J.* C **78** 997
[58] Sirunyan A M *et al* (CMS Collaboration) 2017 *Phys. Rev. Lett.* **119** 152301
[59] Sirunyan A M *et al* (CMS Collaboration) arXiv:1810.03022
[60] Aaboud M *et al* (ATLAS Collaboration) 2018 *Eur. Phys. J.* C **78** 762
[61] Khachatryan V *et al* (CMS Collaboration) 2017 *Eur. Phys. J.* C **77** 252
[62] Sirunyan A M *et al* (CMS Collaboration) arXiv:1810.11102
[63] Aaboud M *et al* (ATLAS Collaboration) 2018 *Eur. Phys. J.* C **78** 784
[64] Jaelani S and (ALICE Collaboration) 2018 *J. High Energy Phys.* JHEP10(2018)174
[65] Sirunyan A M *et al* (CMS Collaboration) 2018 *Phys. Lett.* B **782** 474
[66] Sirunyan A M *et al* (CMS Collaboration) 2018 *Phys. Rev. Lett.* **120** 202301
[67] Molnar D and Sun D 2014 *Nucl. Phys.* A **932** 140
Molnar D and Sun D 2013 *Nucl. Phys.* A **910–911** 486
[68] Renk T 2012 *Phys. Rev.* C **85** 044903
[69] Bjorken J D 1983 *Phys. Rev.* D **27** 140
[70] Kolb P F and Heinz U W *Quark Gluon Plasma* ed R C Hwa *et al* (Singapore: World Scientific) pp 634–714 [nucl-th/0305084]
[71] Djordjevic M, Stojku S, Djordjevic M and Huovinen P arXiv:1903.06829 [hep-ph]